AIAA-2002-0195

FLAME RESPONSE TO EXCITATION AT FREQUENCIES <60 Hz AS MEASURED BY PHASE-RESOLVED NO PLIF

A. Ratner, S.L. Palm, W. Pun, B. Ramirez, and F.E.C. Culick
California Institute of Technology
Pasadena, CA

40th AIAA Aerospace Sciences
Meeting & Exhibit

14-17 January 2002 / Reno, NV

FLAME RESPONSE TO EXCITATION AT FREQUENCIES <60 Hz AS MEASURED BY PHASE-RESOLVED NO PLIF

Albert Ratner*, Steven L. Palm†, Winston Pun‡, Brenda Ramirez§, and F.E.C. Culick**
Graduate Aeronautical Laboratories and Department of Mechanical Engineering
California Institute of Technology
Pasadena, CA 91125

Abstract – The California Institute of Technology's Combustion Acoustics Facility is used to measure the changes in the creation of NO in a partially premixed jet flame due to acoustic forcing at frequencies ranging from 22 to 55 Hz. The facility generates a quarter-wave mode so that the test flame is in a region where the acoustic velocity is nearly zero. This facility and a similar burner have been previously used to measure the phase-resolved response of the OH field. In this experiment, phase-resolved NO planar laser-induced fluorescence (PLIF) measurements are recorded. The location and phase coupling of the NO field are analyzed, and the production and transport of NO are compared with previously reported OH field measurements. The NO levels increase for frequencies that exhibit stronger acoustic coupling to the flame. The NO concentration field variations lead (in phase space) the OH field variations. This is probably a result of the greater NO sensitivity to temperature (which itself is closely coupled to the chamber pressure).

INTRODUCTION

Increasing consumption of fossil fuels has created a variety of environmental problems that science has to continually battle. As current problems are solved, new ones appear. This has been especially true of Nitric Oxide (NO_x). NO_x is a pollutant produced in common combustion processes. For the continued reduction in the amount of NO_x produced, it is essential that the chemical mechanisms that lead to NO production (and subsequently to NO_x) be well understood. In some combustion environments, there has been substantial progress.

Hanson and coworkers[1] have spent over 15 years examining NO by planar laser-induced fluorescence (PLIF) and the possibility of measuring NO concentrations as an indicator of other parameters[2]. A significant amount of work has also been conducted on NO kinetics[3]. The performance of the most common type of NO Laser-Induced fluorescence (LIF), at 226 nm, has been extensively examined, including the characterization of radiative lifetimes and quenching[4]. Its behavior at elevated pressures has been quantified[5] as well as the performance of LIF at 226 nm versus other methods[6] and excitation frequencies[7].

On the other hand, little work has been presented on NO formation in acoustically active environments. Acoustically active combustion environments are of interest because they already occur in gas turbine combustors that are currently in use. Also, as fuel mixtures are made leaner, acoustic problems typically worsen. There are hypotheses that have been proposed to explain some of the NO production behavior that has been seen in engines. Unfortunately, there has been no conclusive

---

* Postdoctoral Scholar, Graduate Aeronautical Laboratories, Member AIAA
† Graduate Student, Graduate Aeronautical Laboratories, Member AIAA
‡ Postdoctoral Scholar, Department of Mechanical Engineering, Member AIAA
§ Undergraduate Research Fellowship Student, Graduate Aeronautical Laboratories
** Richard L. and Dorothy M. Hayman Professor of Mechanical Engineering and Professor of Jet Propulsion, Fellow AIAA

experimental data to show what the proper mechanism is and how it behaves. Even in the absence of coherent acoustic oscillations, the production of NO is a dynamical process. Hence knowledge gained from the experiments reported here will help clarify behavior at a more fundamental level.

The purpose of this work is to examine NO production in a partially premixed flame under acoustically active conditions. These data will then be compared to OH field data that were obtained in a similar configuration[8,9]. This should provide an indication as to whether NO appears in high temperature zones (as indicated by high OH concentration levels). This should also be indicated by the amount NO leads or lags the OH as the phase of the pressure varies.

CONFIGURATION OF EXPERIMENTAL APPARATUS

The burner utilized for this experiment is located inside an acoustic chamber in which individual frequency bulk modes are generated. The configuration of the acoustic test chamber is shown in Figure 1. The acoustic driving system is located in the upper portion of the chamber. The upper portion is made of a large tubular stainless steel section, in the shape of a cross, approximately 30.5 cm in diameter and 71 cm in height. The exhaust section is open to the atmosphere, providing an acoustically open exit condition. A pair of acoustic drivers are sealed to a pair of air jet film cooling rings (to prevent heat failure of the drivers), which are in turn sealed to opposite sides of the steel structure. The acoustic chamber has an aluminum ring at the bottom, creating a closed-end acoustic condition. It has two sets of inlet louvers cut on opposing sides to allow air to flow into the tube, while maintaining acoustic closure. A large quartz tube rests in a thin register on the aluminum ring, and extends 1.1 m to the driver section. The total height of the chamber is approximately 1.78 m.

The acoustic drivers are 30.5 cm diameter subwoofers with a continuous power handling capacity of 400 W. A 1000 W power amplifier and a function generator provide the power and signal to the acoustic drivers. The amplitude of the fundamental driving mode is actively controlled by custom-designed electronics, which measure the pressure in the acoustic chamber at the burner with a pressure transducer, and appropriately scale the power output of the speakers. The piezoelectric pressure transducer is located at a height of 7.62 cm above the fuel spud, where the flame is stabilized in the burner. This transducer was selected for its high sensitivity (493.3 mV/psi) and thermal characteristics. The signal from the transducer is notch-filtered to ensure the intended driving mode is correctly amplified or attenuated.

The burner consists of a fuel jet, an eductor block, and a flame enclosure (Figure 1). The fuel jet entrains air and partially premixes as it passes through the eductor. The flame is stabilized in the low velocity zone created as the flow exits the eductor, and expands into the burner tube. The fuel jet is 0.428 cm in diameter and is located 2 cm below the eductor block. The eductor is 4.5 cm in height, has a 3.6 cm throat diameter, and is made of high temperature ceramic. A square-profile fused silica burner tube mounts on top of the ceramic eductor. The tube is 11.43 cm in height and 5.72 cm in length on each side. The fuel jet is 50% methane premixed with 50% N_2 gas to increase the mass flow and produce a permanently blue flame. A blue flame (with no soot or soot precursors) is necessary because the black-body radiation from solid particles would over-whelm the weak signal that is being measured for NO PLIF. The premixer inlets for each gas are choked, in order to prevent disturbances from propagating upstream and affecting flow rates.

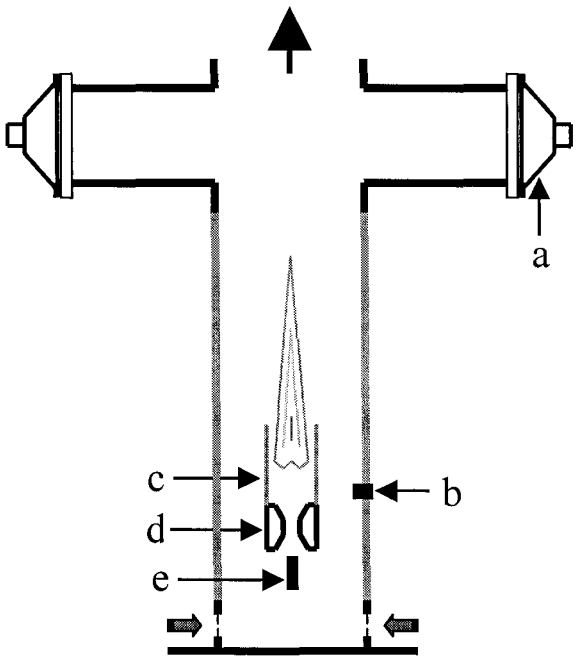

Figure 1. Schematic of test chamber and burner assembly; some of the components are (a) acoustic driver, (b) pressure transducer, (c) fused-silica burner tube, (d) eductor block, and (e) fuel spud.

The PLIF system (Figure 2) is based on an Nd:YAG laser operating at 10 Hz, pumping a tunable dye laser, which in turn drives a mixer/doubler system. The Nd:YAG laser outputs 2000 mJ/pulse at 1064 nm (IR), and is equipped with a secondary harmonic generation system to provide 1000 mJ/pulse at 532 nm (green). Shot-to-shot laser energy is measured for each pulse with an energy meter. Rhodamine 590/610 in methanol is used as the dye laser mixture to produce 574 nm (> 200 mJ/pulse), which is then doubled to 287 nm and mixed with the 1064 nm beam to approximately 226 nm. The 226 nm laser beam is narrowed using a plano-concave cylindrical lens (radius of curvature = 100 mm), and spread into a sheet in the plane at 90° to the converging plane by a plano-convex cylindrical lens (radius of curvature = 25.43 mm). Approximately 4 to 5 mJ/pulse of energy are provided by this system into the test section to stimulate NO, resulting in saturated fluorescence.

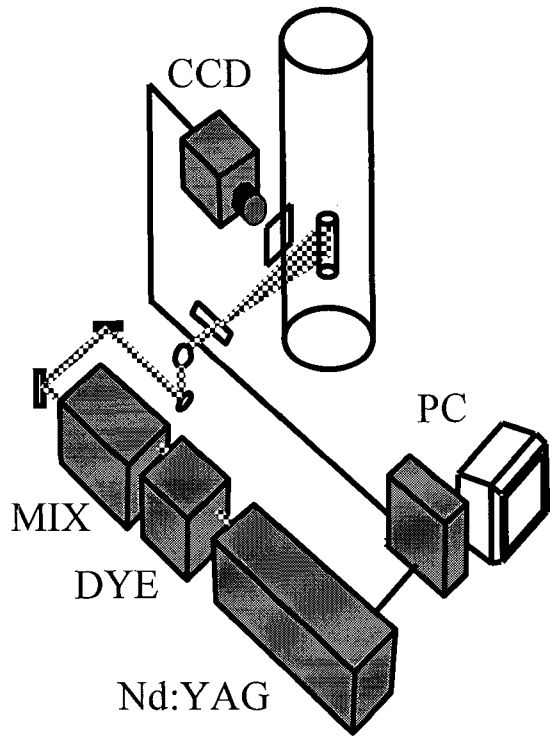

Figure 2. Schematic of the PLIF and CCD camera system, including a Nd:YAG laser, a tunable dye laser, and a frequency mixer/doubler.

The detector for the fluorescence signal is an intensified CCD camera, using a 512x512 CCD array, operated with a gate width of 200 ns. The thin UV sensitive coating on the photocathode does not allow the intensifier to be gated quickly. Due to the requirement of high QE and fast gating, the microchannel plate (MCP) of the camera is therefore gated. Attached to the camera is a catadioptric all-reflective F/1.2 UV lens with a focal length of 105 mm. The lens provides high light throughput while minimizing spherical and chromatic aberrations. To improve the signal-to-noise ratio, pixels were binned 2x2 on-chip. This results in a spatial resolution of 357 μm x 357 μm per pixel at the focal plane, with a 256x256 pixel image, resulting in a focal plane image size of 83.6 cm^2.

DATA REDUCTION

The key assumption for this work is that the flame responds in a periodic fashion to the periodic acoustic forcing. Taking advantage of this periodicity, the PLIF images are phase-binned and averaged together, to generate the periodic response of the NO fluorescence in the flame. As previously mentioned, the oscillating pressure used to phase-resolve the images is acquired by a pressure transducer located 8 cm above the fuel spud, in the zone where the flame is stabilized. Using a phase preserving filter, the transducer signal is filtered about the fundamental driving frequency to produce a clean signal with which to perform the phase-binning process. Each image is placed in an appropriate bin, based on the position of the incident laser shot (and subsequent camera trigger) relative to the rising edge zero crossing of the pressure signal. This process is illustrated schematically in Figure 3, using 8 bins, while in the actual data analysis, 36 bins are used. The top portion of Figure 3 shows a laser shot occurring at a phase angle of ϕ (with the shot labeled as the letter (a). The PLIF image that corresponds to this laser shot is then sorted into its appropriate bin (as shown be the bottom portion of Figure 3) and all of the images in each bin are averaged together.

Due to the distributed nature of the flame being studied and limitations on the ICCD camera's field of view, multiple sets of images were taken at each test condition at different heights. Each case contains a total of over 1000 images, phase-averaged into 36 equally spaced bins. Statistics indicate an even distribution among the bins, with approximately 30 images per bin. The averaged background is subtracted in each bin to eliminate scattering effects from the laser, and corrections are made for variations in spatial and shot-to-shot beam intensity. Images at the same phase but different heights are then matched geometrically, and their intensities

adjusted to match in the overlap region using a least-squares minimization routine. This is the same procedure as that employed for the previously obtained OH PLIF images[8].

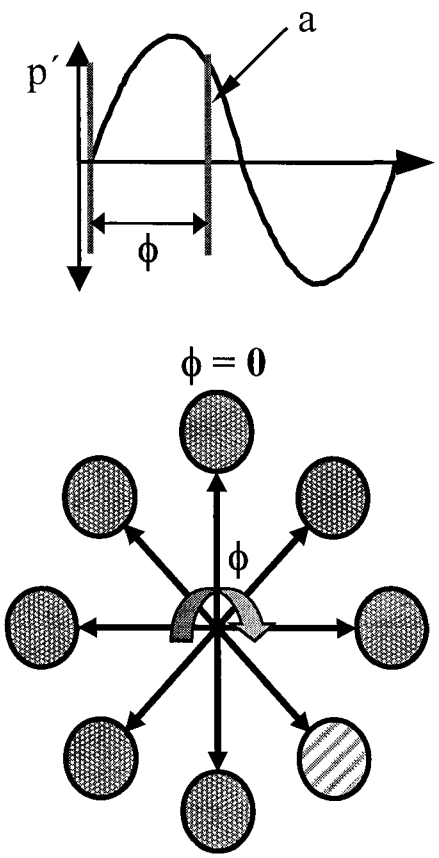

Figure 3. Phase-binning procedure for NO PLIF images. The top graph shows a laser pulse (a) occurring at a phase angle of ϕ. The resulting image is then sorted into its appropriate phase bin.

RESULTS AND DISCUSSION

The response in the production of NO was measured for five different frequencies, 22 Hz, 27 Hz, 32 Hz, 37 Hz, and 55 Hz. The data has been smoothed so that it is easier to plot and interpret. Figure 4 shows the mean NO PLIF response to a driving frequency of 32 Hz at 12 different times during an acoustic period. For comparison, Figure 5 shows the OH PLIF response at 32 Hz. Several regions in the NO images exhibit acoustic coupling. Above the quartz tube (from 9 cm to 11 cm), a distinct puffing pattern can be seen. The minimum horizontal span of the 10% of peak contour occurs at approximately 90° of pressure phase (Figure 4). The horizontal span then continuously increases to a maximum at approximately 270°; after which it shrinks to its initial size. As expected, the behavior of the horizontal span of this contour closely follows the phase behavior of the pressure in its variation. The pressure oscillations follow a sine curve, with a peak at 90° of phase and a low at 270°.

The expectation is that as pressure drops outside the quartz tube, the flame should expand outwards at the tube exit, and the reverse should occur as the pressure increases. This behavior is visible in the horizontal span oscillation described previously. It also follows that there should be an associated characteristic flow time. If the frequency is too low, then the change in pressure is slow enough that the flame can come to equilibrium with almost no visible change. If the frequency is too high, then the flame can't respond fast enough, and again there is little detectable change. Over a certain central band of frequencies, the flame will exhibit its maximum response. The maximum response of the horizontal span of the 10% contour between 9 and 11 cm high is 6.5%, 9.3%, 9.8%, 6.7%, and 2.2% for 22, 27, 32, 37, and 55 Hz respectively (absolute error is <20% of value and relative error is <10% of value). The flame at the top of the burner tube responds strongest to approximately 30 Hz. The correlation of the data with expected behavior implies that the NO field is responding to acoustic forcing in a predictable and detectable way.

It is also useful to compare the images of the NO concentration in Figure 4 to the corresponding OH field images (Figure 5). For example, between 9 and 11 cm in height, an increase in NO concentration correlates with a decrease in OH. At first glance, this seems counter-intuitive because NO and OH concentration should increase together. This is not the case at this height because NO is not being produced, but transported. As the flame emerges from the quartz tube, it mixes with the surrounding cold air. The cooling greatly reduces the amount of OH, but has no impact on NO that already exists. Hence, the larger the span of the NO zone, the more mixing with cold external air that has occurred. So, when the mixing is greatest, it results in the widest distribution of NO and the least amount of OH (which can be seen on the 90° images of both NO and OH). The next step is to quantify the global NO response and to compare that to the previously measured OH response at these frequencies.

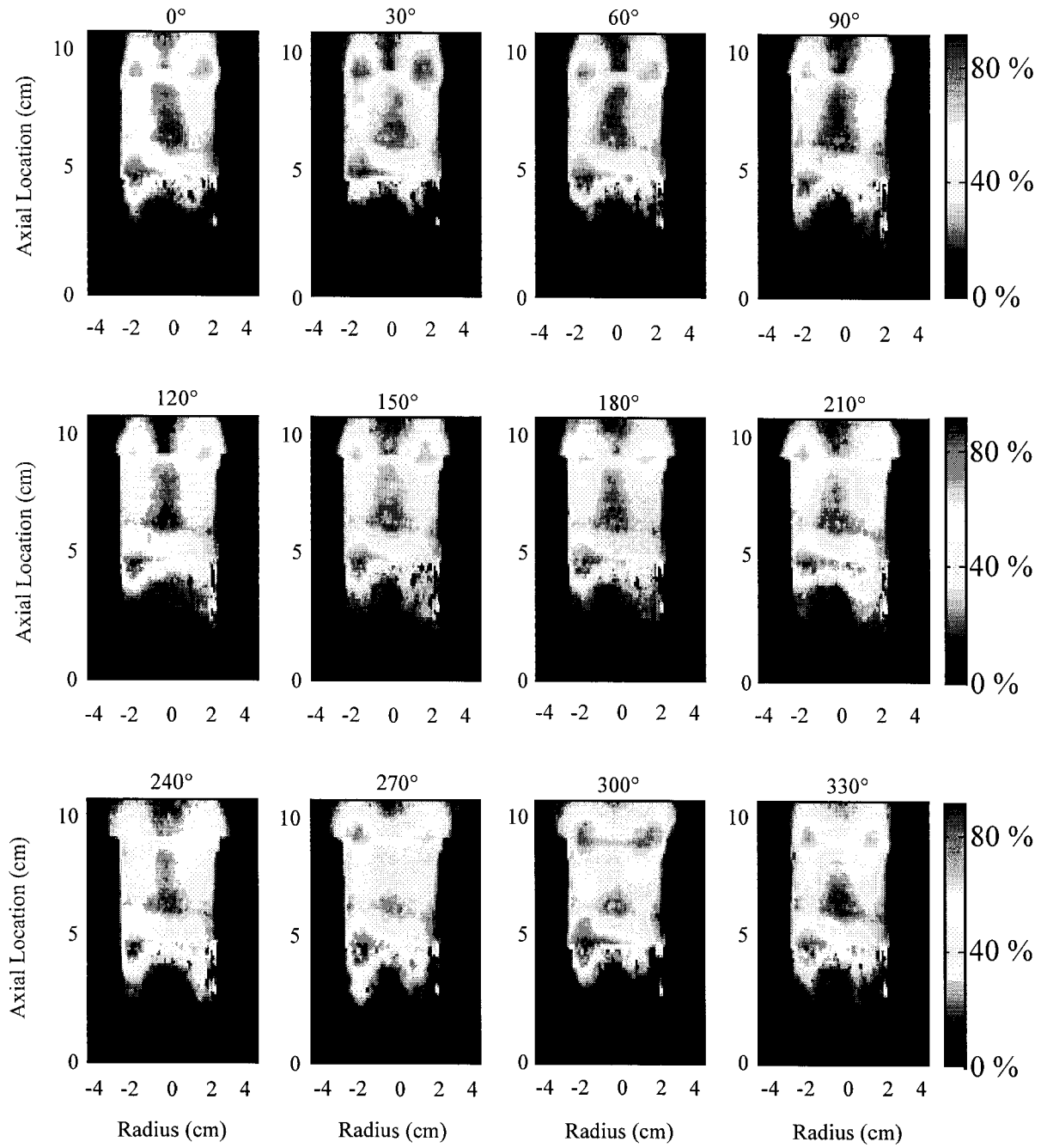

Figure 4. NO PLIF images over a period of a sinusoidal pressure oscillation at 32 Hz. The intensity scale is percentage of peak signal.

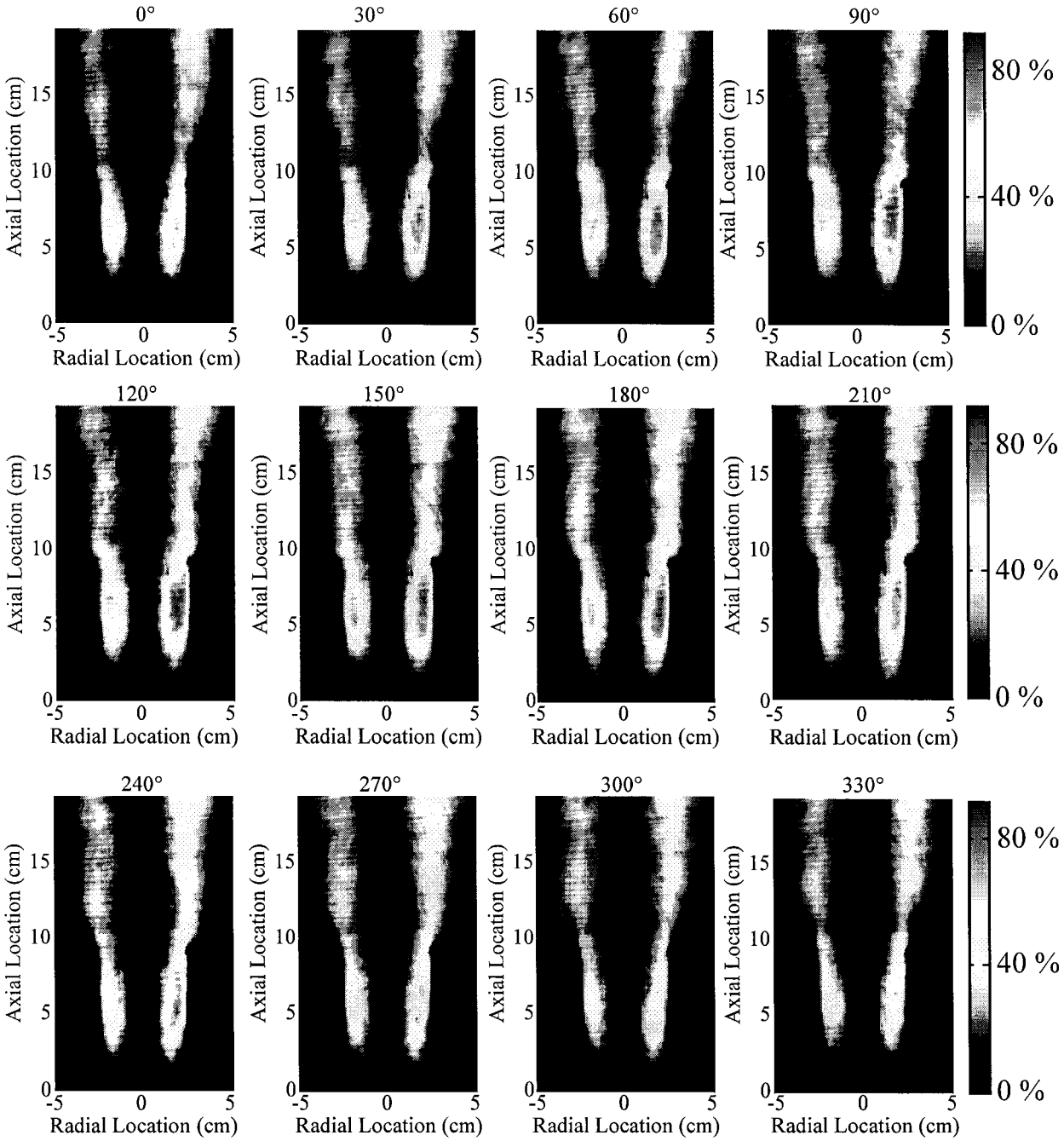

Figure 5. OH PLIF images over a period of a sinusoidal pressure oscillation for the aerodynamically stabilized burner at 32 Hz (Pun[9]).

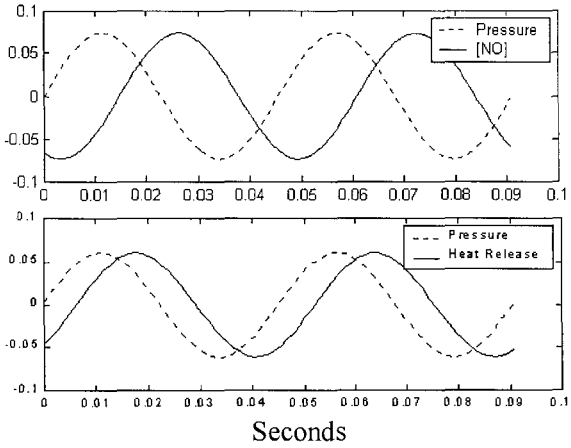

Figure 6. Phase lag of NO (top) and heat release as calculated from OH (bottom, from Pun[9]). (Concentrations in arbitrary units)

Figure 6 shows global NO variation and its phase shift from the pressure oscillation. Both the NO and pressure signals have been filtered to remove harmonics. For NO, the harmonics are 10% of the fundamental frequency or smaller for 22 to 32 Hz. For 37 and 55 Hz significant harmonic content is observed, but the magnitude of the overall response is low, with the harmonics still mostly less than 10% of the amplitude of the fundamental frequency at 22, 27, and 32 Hz. The pressure signal has significant harmonic content at 22 Hz, when the amplitude of the 3rd harmonic is 50% of the fundamental. At 27 Hz, the amplitude of the strongest higher harmonic is down to 10%, and falls off to less than 3% for the higher frequencies.

Table 1 shows that the phase lag between the pressure and the NO is approximately constant, while the lag for OH increases as the frequency increases. This can be understood as a result of the NO response being fast relative to the driving signal, while the OH response is slow. For example, at 55 Hz the time available for a response is half that of 27 Hz. Hence, the first half of the OH response at 55 Hz is very similar to the first quarter of the response at 27 Hz. After that, unlike the case at 27 Hz, at 55 Hz the pressure is decreasing. Since the OH concentration builds up slowly, it reaches detectable levels at a later time for the higher frequency cases (significantly later as a function of phase). The NO response is fast, with the peak magnitude between 107° and 141° of phase after the pressure peak for all cases.

	22 Hz	27 Hz	32 Hz	37 Hz	55 Hz
[NO] PHASE LAG (°)	115	129	108	141	126
[NO] MAG. (%)	7.1	9.1	11.9	8.4	13.8
[OH] PHASE LAG (°)	52	56	76	118	187
[OH] MAG. (%)	4.9	5.8	11.5	10.3	2.3

Table 1. Phase lag and oscillation magnitude of the NO and OH concentrations.

CONCLUSIONS

The data presented in this paper show that acoustic coupling in the flame investigated here can cause higher NO production levels than would have occurred without the presence of acoustic waves. This indicates that a modified design that reduces the acoustic coupling of this system would likely result in reduced NO production. This will be examined in future work since a method already exists for reducing the acoustic response of this flame (Pun[9]).

It has also been demonstrated that NO fluctuations can be measured in a realistic system. This work was performed on a system that has both partial premixing of the fuel and some flame enclosure components. The environment was acoustically active and the flame was unsteady both spatially and temporally. The ability to acquire quantitative measurements in this test rig indicates that the method should be applicable to configurations closer to those used in practical combustion systems.

The data is also valuable because it provides a benchmark for computer models. Partially premixed flames in acoustically forced conditions are difficult to model, due to the inherent difficulties in capturing the correct physics as well as the lack of a validation database. These measurements, along with the OH PLIF and chemiluminescence data that were recently acquired, will provide the basis for significant progress in modeling a greater range of phenomena occurring in realistic combustors.

ACKNOWLEDGEMENTS

The authors thank the L. A. County Sanitation District, the DOE Advanced Gas Turbine Systems Research program, the Air Force Office of Scientific

Research, and the California Institute of Technology for their support of this work.

REFERENCES

1. Hanson, R.K., Seitzman, J.M., and Paul, P.H., Appl. Phys. B 50:441 (1990).
2. McMillin, B.K., Palmer, J.L., Antonio, A.L., and Hanson, R.K., AIAA-92-3347 (1992).
3. Steele, R.C., Malte, P.C., Nicol, D.G., and Kramlich, J.C., Combust. Flame 100:440 (1995).
4. McDermid, I.S. and Laudenslager, J.B., J. Quant. Spectrosc. Radiat. Transfer 27:483 (1982).
5. Allen, M.G., McManus, K.R., and Sonnenfroh, D.M., AIAA-95-0172 (1995).
6. Ravikrishna, R.V., Partridge Jr., W.P., and Laurendeau, N.M., Comb. Sci. and Tech. 144:79 (1999).
7. Schulz, C., Sick, S., Heinze, J., and Stricker, W., Appl. Optics 36:3227 (1997).
8. Pun, W., Palm, S.L., and Culick, F.E.C., AIAA-2000-3123 (2000).
9. Pun, W., Ph.D. Thesis, California Institute of Technology (2001).